

# Photorefractivity in a Novel Polymer Composite with High Diffraction Efficiency and Broad Optical Transparency

Yiping Cui, Bogdan Swedek, Ning Cheng, Kie-Soo Kim, and Paras N. Prasad\*

Photonics Research Laboratory, State University of New York at Buffalo, Buffalo, New York 14260

Received: October 22, 1996<sup>®</sup>

A novel photorefractive polymer composite has been developed in which a new organic dye, 4-[*N*-(2-hydroxyethyl)-*N*-methylamino]-4'-[(6-hydroxyhexyl)sulfonyl]stilbene, is used as a second-order nonlinear optical chromophore together with poly(*N*-vinylcarbazole) as the hole-transporting matrix, tricresyl phosphate as a plasticizer, and C<sub>60</sub> as a photosensitizer. The photoconductive, electro-optic, and photorefractive properties of the material have been experimentally studied at wavelengths of 488, 514.5, and 632.8 nm. The amplitude and the phase dependencies of the electro-optic response have been investigated. The composite shows high photorefractivity over a broad wavelength range. Diffraction efficiencies between 20% and 40% as well as net two-beam coupling gains of 25–65 cm<sup>-1</sup> have been obtained at wavelengths of 488, 514.5, and 632.8 nm.

## Introduction

The phenomenon of photorefractivity is produced in materials which simultaneously exhibit photoconductive and electro-optic properties.<sup>1,2</sup> Photoconductivity allows formation of an internal space-charge electric field through subsequent combination of photogeneration, transport, and trapping of charge carriers. This space-charge field then creates a change of refractive index due to the electro-optic properties. The resulting manifestation of these processes is light induced refractive index modulation. Photorefractive holograms are generated in the form of refractive index gratings written by the crossing of two laser beams in a medium. They are retrieved by the diffraction of a probe beam. A distribution of the space-charge field replicates a pattern of the incident writing beams. Consequently, recorded gratings can be easily modified or completely erased by illumination with another light pattern. An unusual feature of the photorefractive grating is the phase shift between the intensity pattern (interference of the overlapped beams) and the resulting periodic refractive index modulation. This phase shift gives rise to asymmetric two-beam coupling in which one beam gains intensity and the other one loses intensity. The diffraction efficiency, the two-beam coupling gain coefficients, the speed of writing and erasure, and storage time are typical parameters used as the figures of merit of a given photorefractive material.

Photorefractive polymers have drawn a considerable amount of interest over the past few years, because of their potential as an inexpensive and efficient media for high-density optical data storage, optical amplification, and dynamic image processing. Since first observation of the photorefractive effect in a polymeric material,<sup>3</sup> rapid progress has been made in the development and characterization of new composites<sup>4–16</sup> and in understanding of mechanisms accounting for photorefractivity.<sup>17–21</sup> Large diffraction efficiencies and two-beam coupling gain coefficients far exceeding the absorption losses have been obtained.<sup>22,23</sup> Fast kinetics of photorefractive grating recording and erasure,<sup>24–26</sup> quasi-nondestructive reading,<sup>27</sup> and high-density holographic recording<sup>28</sup> have been reported. Also, an optical correlator built with a photorefractive polymer<sup>29</sup> has been demonstrated. These results reveal that the polymeric photorefractive materials show promise for many photonic applications.

For optical data storage and optical information processing, the wavelength of operation is an important property of the material. Photorefractivity for most of polymeric materials reported so far has been achieved at wavelengths ranging from 633 to 753 nm. A material exhibiting photorefractive response over a broad spectral range is desirable for a number of applications such as multicolor optical image processing. Until now, very few materials have been reported to exhibit photorefractivity at a wavelength shorter than 633 nm.<sup>4,30</sup> In this paper we report an efficient photorefractive behavior in a new polymeric composite observed over a broad wavelength range. This polymer composite contains a new organic dye, 4-[*N*-(2-hydroxyethyl)-*N*-methylamino]-4'-[(6-hydroxyhexyl)sulfonyl]stilbene, abbreviated as APSS, which shows good transparency in the wavelength range of 479–1200 nm.<sup>31</sup> This dye is utilized in composite as the electro-optic chromophore. A charge-transporting polymer, poly(*N*-vinylcarbazole) (PVK), plasticized with tricresyl phosphate (TCP) and photosensitized with C<sub>60</sub>, is used as the host matrix. Experimental investigations of the photoconductivity, amplitude and phase dependencies of the electro-optic response, diffraction efficiency, and two-beam coupling gain coefficient of the composite were performed at the wavelengths of 488, 514.5, and 632.8 nm. We show electro-optic response of this low-*T*<sub>g</sub> (glass transition temperature) composite as a function of frequency of modulation in the range of 1 Hz to 100 kHz. We then discuss contributions of the birefringence modulation and the electro-optic effect to the material's photorefractive response.

## Experimental Section

Photorefractive samples were prepared according to the following procedure: PVK (secondary standard from Aldrich), TCP, and APSS were dissolved in a toluene/cyclopentanone solution saturated with C<sub>60</sub>. The composition of the PVK:TCP:C<sub>60</sub>:APSS was prepared in the mixture by weight of 47.7:47.6:0.2:4.5%. The solution was filtered to 0.2 μm and films were cast onto ITO-coated glass substrates with an etched electrode pattern. Then, the films were allowed to dry slowly (for 24 h) at ambient temperature and subsequently heated to 70 °C for 4 h to ensure complete solvent evaporation. Next, the films were softened, by placing them on a hot plate (ca. 200 °C) for 30 s, and pressed by another ITO-coated glass to produce a sandwich

<sup>®</sup> Abstract published in *Advance ACS Abstracts*, April 15, 1997.

layer arrangement between two ITO-coated glass slides. The film thickness ranged between 150 and 250  $\mu\text{m}$ . The glass transition temperature of the composite was found to fall below 14  $^{\circ}\text{C}$  [our lower detection limit of the differential scanning calorimeter (DSC)]. Finally, the samples were sealed with a UV-curable epoxy to prevent diffusion of atmospheric moisture. The entire procedure of film preparation was performed in a class 100 cleanroom. All other details pertaining to the synthesis and/or purification of components of the discussed photorefractive composite are given elsewhere.<sup>22,25,32</sup>

The UV-vis absorption spectra of the composite were recorded on a Shimadzu UV-3101 spectrometer. The photoconductivity was measured using a simple DC photocurrent technique<sup>33</sup> by applying a DC voltage to the sample and measuring the current component induced by a light excitation through the sample. The waveguide *m*-line technique as well as the near normal transmission measurements performed on the thin film were used to determine refractive indices of the material. The electro-optic properties of the composite were measured on thick samples, 170–200  $\mu\text{m}$ , using the transmission configuration of the ellipsometric technique.<sup>34</sup> The use of thick films eliminated unwanted interference associated with multiple beam reflections,<sup>35</sup> which might lead to overestimation or underestimation of values of electro-optic coefficients. A model TREK 610C high-voltage supply/amplifier allowed application of the poling electric field in the range of 0–55  $\text{V}/\mu\text{m}$  as well as the AC modulating field on the level of 1  $\text{V}/\mu\text{m}$  (1–100 kHz) across a 180  $\mu\text{m}$  thick sample. The magnitude of the AC modulating voltage applied to the sample was measured by using a Tektronix P6015 high-voltage passive probe and a digital lock-in amplifier model SR850 DSP. The modulation in the laser beam was detected by a silicone photodiode coupled with a current/voltage transducer amplifier (UDT TRAMP) and measured by the same lock-in amplifier. In this experiment the response of each electronic device, namely high-voltage supply, high-voltage probe, and transducer amplifier, was determined at each measured frequency to ensure proper characterization of the electro-optic modulation of the composite.

The photorefractive properties of PVK:TCP:C<sub>60</sub>:APSS were verified using the degenerate four-wave mixing (DFWM) and the two-beam coupling (2BC) studies at three different wavelengths, 488, 514.5, and 632.8 nm. In the DFWM experiment, two *s*-polarized writing beams of approximately equal intensities were intersected in the sample at the incidence angles of 49 $^{\circ}$  and 66 $^{\circ}$ , producing gratings with a spacing of about 2.65, 2.80, and 3.44  $\mu\text{m}$  for the three wavelengths, respectively. The corresponding intensities of the writing beams at 488, 514.5, and 632.8 nm were 36, 32, and 60  $\text{mW}/\text{cm}^2$ . A *p*-polarized reading beam, propagating in a direction opposite to one of the writing beams, had the intensities of 0.13, 0.32, and 0.12  $\text{mW}/\text{cm}^2$  at wavelengths under consideration. In 2BC measurements the two writing beams were changed to *p*-polarization, and the intensity of one of them (signal beam) was reduced about 65 times to provide undepleted pumping conditions. The gain of intensity by the signal beam was measured. For both diffraction efficiency and two-beam coupling measurements the corresponding steady-state signal was acquired by computer for 30 s and averaged.

## Results and Discussion

Figure 1 shows the absorption spectra of the unsensitized PVK:TCP:APSS (dashed line) and the C<sub>60</sub>-sensitized PVK:TCP:C<sub>60</sub>:APSS (solid line) composite materials. As one can see, the unsensitized PVK:TCP:APSS composite shows high transparency in the blue and green region of the visible spectrum.

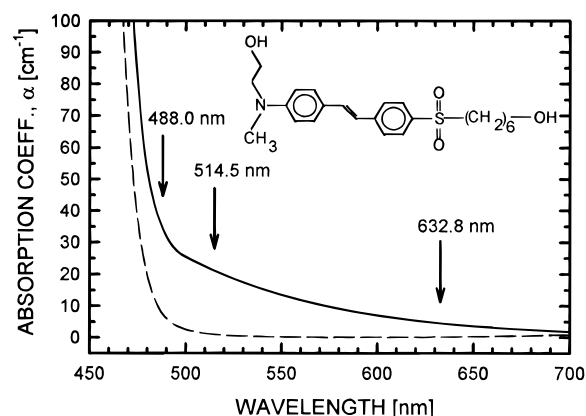


**Figure 1.** Absorption coefficient  $\alpha$  of the unsensitized composite PVK:TCP:APSS (dashed line) and C<sub>60</sub>-sensitized composite PVK:TCP:C<sub>60</sub>:APSS (solid line) as a function of wavelength. The molecular structure of the APSS is shown in the inset.

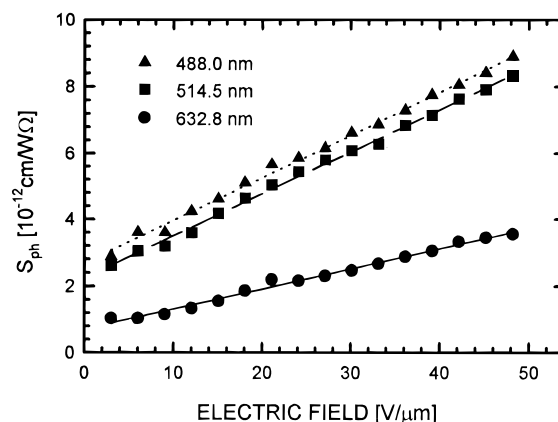


**Figure 2.** Photosensitivity  $S_{\text{ph}}$  versus electric field at three wavelengths. The solid lines are linear fits.

Small absorption of the chromophore assures low background losses of the composite and minimizes formation of non-photorefractive gratings (i.e. photochromic gratings). Upon addition of the photogenerator, C<sub>60</sub> absorption coefficients of the material reach values of 34.5, 21, and 5  $\text{cm}^{-1}$  at the wavelengths of 488, 514.5, and 632.8 nm, respectively.

The electric field dependence of the photosensitivity (photoconductivity per unit light intensity) of the PVK:TCP:C<sub>60</sub>:APSS composite material at the three used wavelengths is shown in Figure 2. The photosensitivity of the composite,  $S_{\text{ph}}$ , is calculated according to the following expression,

$$S_{\text{ph}} = \frac{J_{\text{ph}}}{EP} \quad (1)$$

where  $J_{\text{ph}}$  is the photocurrent density,  $E$  is the applied electric field, and  $P$  is the intensity of illumination of the beam. All dependencies show linear increase with the applied electric field. The photoconductivity at 514.5 nm is 2 times larger than that at 632.8 nm, presumably because of the higher absorption coefficient of C<sub>60</sub> at 514.5 nm than at 632.8 nm. The photoconductivity at 488 nm is close to that at 514.5 nm.

Electro-optic (EO) response is another necessary function for photorefractivity. The glass transition temperature,  $T_g$ , of our composite is lower than room temperature because of the inclusion of the plasticizer TCP. For this reason, it is not necessary to prepoling the sample. The second-order chromophores can be easily aligned by applying a DC electric field without sample heating. Upon application of an electric field,  $E$ , the modulation of the index of refraction of the medium

results from the induced birefringence and from the second-order susceptibility, due to the breaking of inversion symmetry. In the one-dimensional approximation of the chromophore molecule, corresponding refractive index changes for a doped polymer system can be expressed as<sup>20</sup>

$$\Delta n_z^{\text{BR}} = \frac{1}{2n} C_{\text{BR}} E^2$$

$$\Delta n_{x,y}^{\text{BR}} = -\left(\frac{1}{4n}\right) C_{\text{BR}} E^2 \quad (2)$$

$$\Delta n_z^{\text{EO}} = \frac{1}{2n} C_{\text{EO}} E^2$$

$$\Delta n_{x,y}^{\text{EO}} = \frac{1}{6n} C_{\text{EO}} E^2 \quad (3)$$

and coefficients  $C_{\text{BR}}$  and  $C_{\text{EO}}$  are

$$C_{\text{BR}} = \left(\frac{2}{45}\right) N(\alpha_{\parallel} - \alpha_{\perp}) \left(\frac{\mu_z}{k_B T}\right)^2$$

$$C_{\text{EO}} = \frac{N\beta_{zz}\mu_z}{5k_B T} \quad (4)$$

where  $n = n_x = n_y \approx n_z$  is the index of refraction of the composite,  $N$  is the number density of chromophores,  $\alpha_{\parallel}$  and  $\alpha_{\perp}$  are the local field-corrected parallel and perpendicular molecular optical polarizabilities,  $\mu_z$  is the local-field-corrected ground state dipole moment,  $\beta_{zz}$  is the local-field-corrected molecular hyperpolarizability,  $k_B$  is Boltzmann's constant,  $T$  is the absolute temperature, and  $z$  denotes the normal to the sample plane.

We used the well-known transmission ellipsometric technique to study the electro-optic properties of the discussed composite material. In this configuration, the modulation of the refractive index of the sample causes a phase retardation between the  $s$ - and the  $p$ -polarized components of the incident beam, which in turn, after passing through compensator and analyzer, results in intensity modulation which is proportional to the changes in the refractive indices:

$$|\Delta n_z^{\text{BR,EO}} - \Delta n_y^{\text{BR,EO}}| = \frac{1}{2} n^3 E(r_{33}^{\text{BR,EO}} - r_{13}^{\text{BR,EO}}) \quad (5)$$

The measured effective electro-optic coefficient,  $r_{\text{eff}}$ , representing modulation of the refractive index arising from the modulation of birefringence and electro-optic effect, is given by

$$r_{\text{eff}} = r_{33}^{\text{BR,EO}} - r_{13}^{\text{BR,EO}} = \frac{\lambda I_{m,\text{rms}}}{\pi n^2 V_{m,\text{rms}} I_c} \frac{(n^2 - \sin^2(\theta))^{3/2}}{n^2 - 2\sin^2(\theta)} \frac{1}{\sin^2(\theta)} F \quad (6)$$

where  $\lambda$  is the optical wavelength,  $I_{m,\text{rms}}$  is the modulated beam intensity,  $\theta$  is the incident angle of the laser beam,  $V_{m,\text{rms}}$  is the AC modulating voltage applied to the sample,  $I_c$  is the midpoint intensity, and  $F$  is the experimental factor normalizing responses of the high-voltage amplifier, high-voltage probe, and detection transducer at the given frequency of AC modulation. The amplitude behavior of the frequency dependence of the  $r_{\text{eff}}$  of the PVK:TCP:C<sub>60</sub>:APSS is shown in Figure 3 (hollow circles) at a DC electric poling field of 33 V/ $\mu\text{m}$  and the wavelength of 632.8 nm. As one can see, the effective electro-optic activity of the material decreases with the increase of frequency of modulating electric field. It reveals that the contribution to the refractive index modulation in the low-frequency range is

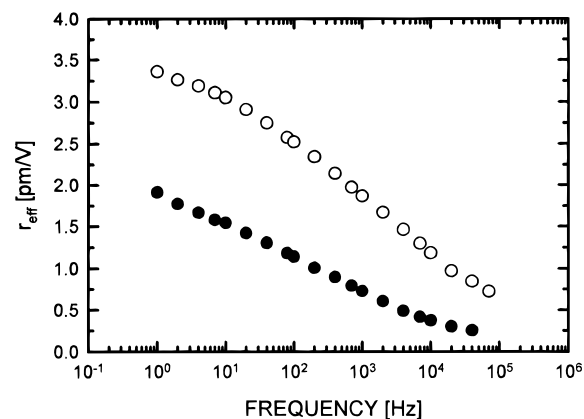


**Figure 3.** Frequency dependence of the amplitude of the effective electro-optic coefficients measured for the two compositions of PVK:TCP:C<sub>60</sub>:APSS containing various amounts of plasticizer (TCP): hollow circles, 47.6 wt %; filled circles, 40 wt %.

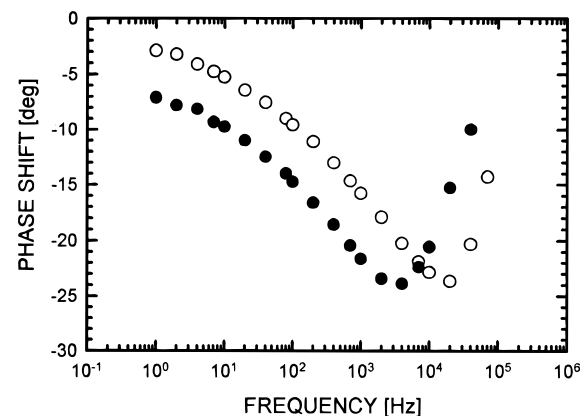


**Figure 4.** Phase shift between the measured optical modulation and the modulating AC electric field as a function of frequency for the two compositions of PVK:TCP:C<sub>60</sub>:APSS containing various amounts of plasticizer (TCP): hollow circles, 47.6 wt %; filled circles, 40 wt %.

predominantly from the reorientation of the chromophores (birefringence contribution, eq 2). Figure 4 displays the behavior of the phase shift, which is defined as the phase deference between the modulating AC electric field and the signal of the modulated light, measured for the same sample (hollow circles). At low frequency, the phase shift is small because the reorientation of the chromophores can follow the AC electric field. At very high frequency, the phase shift is also small because the reorientation time of the chromophores is much longer than the period of the AC field in this frequency range and only a pure electro-optic effect can dominantly contribute to the refractive index modulation. In order to study the orientational mechanism further, we prepared another sample in which the concentration of TCP was reduced to 40 wt % and the concentrations of APSS and C<sub>60</sub> were kept the same as in the previous mixture. As shown in Figure 3 the magnitude of  $r_{\text{eff}}$  of this sample (filled circles) is smaller comparing to the  $r_{\text{eff}}$  of the original composition (hollow circles). A reason for this observation is that orientational mobility of chromophore molecules in more rigid host matrix (containing less amount of plasticizer) is limited; consequently, the modulation of birefringence as well as field-induced second-order susceptibility is smaller than in the composite with 47.6 wt % of TCP. Also the phase shift curve of the harder material in Figure 4 (filled circles), is shifted to the left along the frequency axis, which indicates a longer reorientation time of the chromophore molecules.

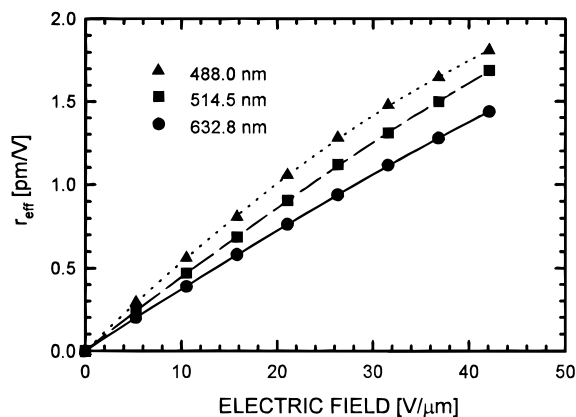


**Figure 5.** Electric field dependence of the effective electro-optic coefficient measured at three different wavelengths. The lines are merely a visual aid.

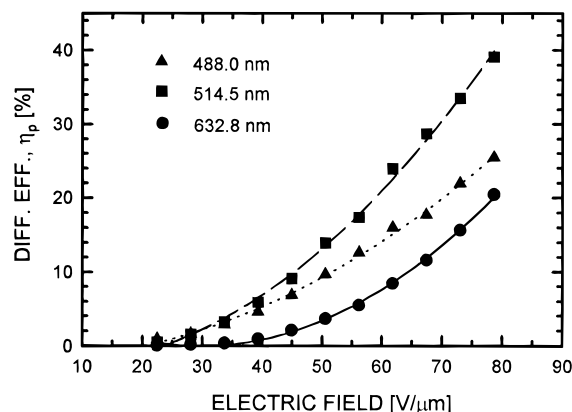


**Figure 6.** Dependence of the steady-state diffraction efficiency in PVK:TCP:C<sub>60</sub>:APSS on electric field at three wavelengths measured on a 180-μm-thick sample. The lines are merely a visual aid.

Figure 5 shows the dependencies of the effective electro-optic coefficients of the PVK:TCP:C<sub>60</sub>:APSS composite on the DC poling field, measured at three wavelengths. The effective electro-optic coefficients of the material follow a sublinear increase with the applied poling field, as theoretically predicted for the electric-field-induced alignment of dipolar chromophores.<sup>36</sup> Also, the magnitudes of the effective electro-optic coefficients are higher at shorter wavelengths. This finding results from the increased anisotropy of the molecular linear polarizability,  $\alpha_{||} - \alpha_{\perp}$ , and the increased hyperpolarizability,  $\beta$ , of the APSS molecules at shorter wavelengths due to dispersion.

The diffraction efficiency of the PVK:TCP:C<sub>60</sub>:APSS composite was measured at three wavelengths of 488, 514.5 and 632.8 nm. Diffraction efficiency is defined as the ratio of intensities of the diffracted and the incident beams. As shown in Figure 6, the diffraction efficiency at 514.5 nm is about twice that at 632.8 nm for an applied electric field of 79 V/μm. There are two reasons for this observation. The higher photosensitivity of the composite at 514.5 nm (see Figure 2) results in a larger number of photogenerated charges, thus a stronger internal space-charge field,  $E_{sc}$ , is created as compared to excitation at 632.8 nm. Consequently higher diffraction efficiency is achieved. The second factor enhancing the diffraction efficiency is a higher effective electro-optic coefficient of the material at shorter wavelengths. As previously discussed in Figure 5, due to dispersion of the linear and the second-order molecular polarizabilities of the chromophore, a more efficient electro-optic activity of the medium is achieved at wavelengths closer to the absorption peak. On the other hand, the diffraction efficiency

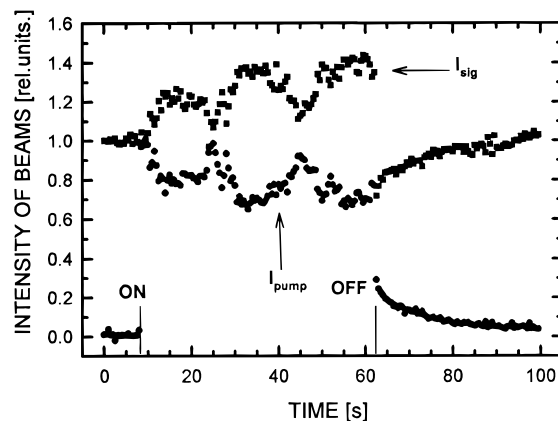


**Figure 7.** Example of asymmetric energy exchange between laser beams in the 2BC experiment recorded at 488 nm in the PVK:TCP:C<sub>60</sub>:APSS photorefractive composite. A poling field of 50 V/μm was applied to the 195-μm-thick sample. The pump beam is open at 8 s and is blocked at 62 s.

at 488 nm is lower than that at 514.5 nm because the sample has higher absorption losses in the reading beam at 488 nm than at 514.5 nm.

Since our photorefractive composite containing only 4.5 wt % of the chromophore exhibits large diffraction efficiencies, one may suspect that the other components of this material (i.e. plasticizer TCP) may contribute to the modulation of the refractive index. In order to study this issue, we have prepared samples without the chromophore, containing similar amounts of remaining components as in the original composite. For a 280-μm-thick film of the PVK:TCP:C<sub>60</sub> mixture and a poling field of 64 V/μm, the diffraction efficiency of  $5 \times 10^{-2}\%$  was measured. Also the effective electro-optic response of this composition was found to be ca. 100 times smaller than the chromophore-doped matrix. These findings indicate a very small contribution of the host matrix to the modulation of the refractive index of discussed composite material.

The characteristic feature of a photorefractive effect is that refractive index grating created in the medium is spatially shifted with respect to the light intensity pattern of the writing beams. As a result an asymmetric energy transfer between beams interfering in a photorefractive sample occurs. Figure 7 shows an example of intensity exchange between the laser beams of equal intensity in a 2BC experiment performed on the PVK:TCP:C<sub>60</sub>:APSS photorefractive sample at the wavelength of 488 nm. In this experiment a DC poling field of 50 V/μm was applied to the sample, and changes in intensity of the interacting beams passing through the sample were simultaneously monitored as one of the beams (pump beam) was open and then blocked. As a photorefractive grating is written, the intensity of the signal beam increases, while the intensity of the pump beam decreases. At the steady-state, the beams exchange about 40% of their relative power. When the pump beam is blocked, part of the remaining signal beam is initially diffracted into the direction of the pump beam. Its uniform illumination, however, erases the previously recorded grating and the signal beam recovers to the original intensity level. The energy transfer between the beams is characterized by the two-beam coupling gain coefficient,  $\Gamma$ , which is calculated according to<sup>2</sup>

$$\Gamma = \frac{1}{D} \ln \left( \frac{gm}{1+m-g} \right) \quad (7)$$

where  $D = L/\cos(\theta)$  is the interaction path for the signal beam ( $L$  = sample thickness,  $\theta$  = propagation angle of the signal beam in the sample),  $g$  is the ratio of intensities of the signal

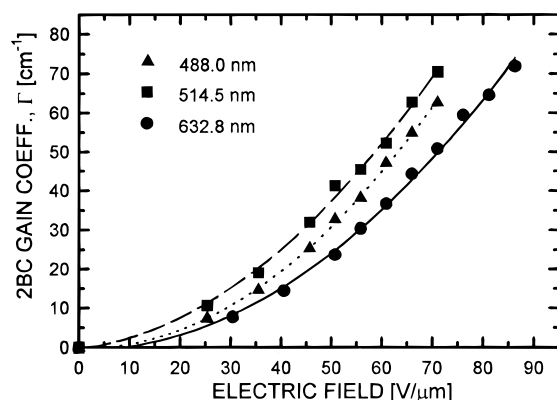


**Figure 8.** Electric field dependence of the steady-state 2BC gain coefficient at the three wavelengths, 488, 514.5 and 632.8 nm. The corresponding absorption coefficients of the sample (glass-ITO-polymer composite-ITO-glass) are 48, 33, and 8 cm<sup>-1</sup>.

beam after the sample with and without the presence of the pump beam, and  $m$  is the ratio of the beam intensities (pump/signal) before the sample. The electric field dependence of the two-beam coupling gain coefficient for the three wavelengths in the PVK:TCP:C<sub>60</sub>:APSS is presented in Figure 8. From a practical perspective of optical amplification,  $\Gamma$  must exceed the absorption loss,  $\alpha$ , of a photorefractive sample. For example, for the sandwiched samples (glass-ITO-polymer composite-ITO-glass) of the PVK:TCP:C<sub>60</sub>:APSS,  $\Gamma - \alpha$ , the net gain coefficients, were 15, 37, and 43 cm<sup>-1</sup>, at a poling field of 71 V/μm, for the wavelengths of 488, 514.5, and 632.8 nm, respectively.

## Conclusions

In conclusion, a new dye, APSS, was used as the chromophore in a photorefractive composite PVK:TCP:C<sub>60</sub>:APSS. The composite containing a low amount of the chromophore shows good photorefractive properties over a wide wavelength range of 488–632.8 nm. The amplitude and phase dependencies of the effective electro-optic response reveal that the photorefractive effect in this composite is significantly enhanced by the modulation of induced birefringence. Owing to higher photosensitivity as well as dispersion of the linear and the second-order polarizabilities, the photorefractive figures of merit of the composite are larger at shorter wavelengths. Efficient two-beam coupling gain coefficients, exceeding absorption losses, have been demonstrated at all used wavelengths.

**Acknowledgment.** The authors thank Dr. Jacek Swiatkiewicz, Ms. M. Li, Mr. M. Yoshida, and Mr. J. Winiarz for their help in this work. This research work was sponsored by the Ballistic Missile Defense Organization and the Chemistry and Life Sciences Directorate of the Air Force Office of Scientific Research through contract numbers F49620-94-10335 and F49620-96-10124. Y.C. would like to acknowledge the National Natural Science Foundation of China for partial support of his research group in China.

## References and Notes

- (1) Gunter, P.; Huignard, J.-P., Eds. *Photorefractive Materials and Their Applications*; Springer-Verlag: Berlin, 1988; I& II, Topics in Applied Physics Vols. 61 and 62.

- (2) Yeh, P. *Introduction to Photorefractive Nonlinear Optics*; Wiley: New York, 1993.
- (3) Ducharme, S.; Scott, J. C.; Twieg, R. J.; Moerner, W. E. *Phys. Rev. Lett.* **1991**, *66*, 1846.
- (4) Moerner, W. E.; Silence, S. M. *Chem. Rev.* **1994**, *94*, 127 (and references therein).
- (5) Sansone, M. J.; Teng, C. C.; East, A. J.; Kwiatek, M. S. *Opt. Lett.* **1993**, *18*, 1400.
- (6) Kippelen, B.; Tamura, K.; Peyghambarian, N.; Padias, A. B.; Hall, H. K., Jr. *J. Appl. Phys.* **1993**, *74*, 3617.
- (7) Yokoyama, K.; Arishima, K.; Shimada, T.; Sukegawa, K. *Jpn. J. Appl. Phys.* **1994**, *33*, 1029.
- (8) Liphardt, M.; Goonesekera, A.; Jones, B. E.; Ducharme, S.; Takacs, J. M.; Zhang, L. *Science* **1994**, *263*, 367.
- (9) Yu, L.; Chan, W.; Bao, Z.; Cao, S. X. F. *Macromolecules* **1993**, *26*, 2216. Yu, L. P.; Chen, Y. M.; Chan, W. K.; Peng, Z. H. *Appl. Phys. Lett.* **1994**, *64*, 2489.
- (10) Zhang, Y.; Spencer, Ch. A.; Ghosal, S.; Casstevens, M. K.; Burzynski, R. *Appl. Phys. Lett.* **1994**, *64*, 1908.
- (11) Silence, S. M.; Donckers, M. C. J. M.; Walsh, C. A.; Burland, D. M.; Twieg, R. J.; Moerner, W. E. *Appl. Opt.* **1994**, *33*, 2218.
- (12) Prasad, P. N.; Orczyk, M. E.; Swedek, B.; Zieba, J.; Zhao, C.-F.; Park, C.-K.; Burzynski, R.; Zhang, Y.; Ghosal, S.; Casstevens, M. K. *Proc. SPIE* **1995**, *2527*, 230.
- (13) Malliaras, G. G.; Krasnikov, V. V.; Bolink, H. J.; Hadzioannou, G. *Appl. Phys. Lett.* **1995**, *66*, 1038.
- (14) Zhao, C.-F.; Park, C.-K.; Prasad, P. N.; Zhang, Y.; Ghosal, S.; Burzynski, R. *Chem. Mater.* **1995**, *7*, 1237.
- (15) Zhang, Y.; Ghosal, S.; Casstevens, M. K.; Burzynski, R. *J. Appl. Phys.* **1996**, *79*, 8920.
- (16) Zhang, Y.; Burzynski, R.; Ghosal, S.; Casstevens, M. K. *Adv. Mater.* **1996**, *8*, 111.
- (17) Ducharme, S.; Jones, B.; Takacs, J. M.; Zhang, L. *Opt. Lett.* **1993**, *18*, 152.
- (18) Sandalphon; Kippelen, B.; Peyghambarian, N.; Lyon, S. R.; Padias, A. B.; Hall, H. K. Jr. *Opt. Lett.* **1994**, *19*, 68.
- (19) Silence, S. M.; Bjorklund, G. C.; Moerner, W. E. *Opt. Lett.* **1994**, *19*, 1822.
- (20) Moerner, W. E.; Silence, S. M.; Hache, F.; Bjorklund, G. C. *J. Opt. Soc. Am. B* **1994**, *11*, 320.
- (21) Orczyk, M. E.; Zieba, J.; Prasad, P. N. *Appl. Phys. Lett.* **1995**, *67*, 311.
- (22) Orczyk, M. E.; Swedek, B.; Zieba, J.; Prasad, P. N. *J. Appl. Phys.* **1994**, *76*, 4995.
- (23) Meerholz, K.; Volodin, B. L.; Sandalphon; Kippelen, B.; Peyghambarian, N. *Nature* **1994**, *371*, 497.
- (24) Silence, S. M.; Walsh, C. A.; Scott, J. C.; Matray, T. J.; Twieg, R. J.; Hache, F.; Bjorklund, G. C.; Moerner, W. E. *Opt. Lett.* **1992**, *17*, 1107.
- (25) Orczyk, M. E.; Zieba, J.; Prasad, P. N. *J. Phys. Chem.* **1994**, *98*, 8699.
- (26) Malliaras, G. G.; Krasnikov, V. V.; Bolink, H. J.; Hadzioannou, G. *Appl. Phys. Lett.* **1994**, *65*, 262.
- (27) Silence, S. M.; Twieg, R. J.; Bjorklund, G. C.; Moerner, W. E. *Phys. Rev. Lett.* **1994**, *73*, 2047.
- (28) Moerner, W. E.; Poga, C.; Jia, Y.; Twieg, R. J. In *Organic Thin Films For Photonics Applications Technical Digest*, 1995; Vol. 21 Optical Society of America: Portland, OR, 1995; pp 330–333.
- (29) Halvorson, C.; Kraabel, B.; Heeger, A. J.; Volodin, B. L.; Meerholz, K.; Sandalphon; Peyghambarian, N. *Opt. Lett.* **1995**, *20*, 76.
- (30) Burzynski, R.; Zhang, Y.; Ghosal, S.; Casstevens, M. K. *J. Appl. Phys.* **1995**, *78*, 6903.
- (31) He, G. S.; Bhawalkar, J. D.; Zhao, C.-F.; Park, C.-K.; Prasad, P. N. *Opt. Lett.* **1995**, *20*, 2393.
- (32) Kim, K.-S. Manuscript in preparation.
- (33) Schildkraut, J. S.; *Appl. Phys. Lett.* **1991**, *58*, 340.
- (34) Teng, C. C.; Man, H. T. **1990**, *56*, 1734.
- (35) Schildkraut, J. S.; *Appl. Opt.* **1990**, *29*, 2839.
- (36) Prasad, P. N.; Williams, D. J. *Introduction to Nonlinear Optical Effects in Polymers and Molecules*; Wiley: New York, 1991.